The excited states of iodide anions in water: a comparison of the electronic structure in clusters and in bulk solution

Stephen E. Bradforth[1],* and Pavel Jungwirth[1,2]

[1] *Department of Chemistry, University of Southern California,*
Los Angeles, CA 90089-0482 U.S.A.
bradfort@usc.edu, fax: +1 (213) 740-0461

[2] *J. Heyrovský Institute of Physical Chemistry, Academy of Sciences of the Czech Republic and*
Center for Complex Molecular Systems and Biomolecules, Dolejškova 3,
18223 Prague 8, Czech Republic
jungwirt@jh-inst.cas.cz, fax: +420 2-8582307

Abstract:

A new computational approach for calculating charger-transfer-to-solvent (CTTS) states of anions in polar solvents is presented. This is applied to the prototypical aqueous iodide system when the anion is placed in the interior or at the gas-liquid interface of a bulk water solution or hydrated in small gas phase clusters. The experimental vertical detachment energies and CTTS transition energies are quantitatively reproduced without any adjustable parameters. The representative shapes of bulk CTTS wavefunctions are shown for the first time and compared with cluster excited states. The calculations start with an equilibrium classical molecular dynamics simulation of the solvated anion allowing for an extended sampling of initial configurations. In the next step, ab initio calculations at the MP2 level employing an extended diffuse basis set are performed for the anionic ground and lowest triplet state, as well as for the corresponding neutral system. It is argued that due to the small singlet-triplet splitting, the triplet state is a good model for the experimental CTTS state. The present calculations on aqueous

iodide ion are made computationally feasible by replacing all water molecules (or all waters except for the first solvation shell) by fractional point charges. It is concluded that the bulk wavefunction is mainly defined by the instantaneous location of voids in the first solvation shell, which arise due to thermal disorder in liquid water. The key ingredient to CTTS binding in the bulk is the long-range electrostatic field due to the pre-existing polarization of water molecules by the ground state iodide ion. This is very different from the situation in small water clusters, where the CTTS state is an order of magnitude more fragile due to the lack of long-range polarization. Therefore, it is argued that the electronic structure of small halide clusters cannot be directly extrapolated to the bulk.

1. Introduction

Aqueous halide anions exhibit intense absorption bands in the deep ultraviolet. The transition energies for these bands are strongly dependent on solvent, temperature and perturbations to the solvent environment surrounding the anion (*e.g.,* addition of salt, sucrose or co-solvent).[1] Because these electronic bands are absent in the isolated gas phase ion, the transitions responsible for this absorption are assigned as charge-transfer-to-solvent (CTTS). For aqueous I^-, the lowest CTTS band component rises around 260 nm and peaks at 225 nm (5.5 eV).[1,2] The vertically excited state is believed to have the promoted electron spatially extended over the solvent shell but still centered on the iodine atom.[3,4] The CTTS state is quasi-bound; excitation into the iodide band is accompanied by the production of solvated electrons.[3,5] There is a long history of attempts dating back to work by Franck in the 1920's to understand the nature of these bands[6] and, with the discovery of the hydrated electron in 1960's,[7] to understand how the structure of the excited state relates to the mechanism for appearance of a solvated electron.

Recent experiments[8-11] on aqueous iodide have shown that, in accord with mixed quantum/classical molecular dynamics simulations,[12] electron transfer proceeds within 200 fs from the excited anion into a nearby cavity site in the surrounding solvent to form a solvated electron.

Two simple models have traditionally been invoked to describe the CTTS phenomenon. The first emphasized that the electron is bound by the existing long-range polarization of the solvent at the instant of excitation. This model was advanced by Platzmann and Franck and refined as the "diffuse" model by Treinin and coworkers.[2,4,13,14] The alternative model concentrates on the confinement of the promoted electron within the solvent cavity surrounding the anion.[15,16] The confinement is due to the repulsion of the CTTS electron by the solvent electrons that leads to a simple particle in a box picture for the excess electron. This "confined" model is rather similar to the description of F-centers in alkali halide glasses and crystals and to the solvated electron in water.[17] Notice that neither model concerns itself with the central iodine atom which is a spectator and simple thermodynamic formulae are required to predict the energy of the CTTS band.[4,13] Such thermodynamic cycles do correctly predict CTTS bands in several inorganic anions and coordination compounds[18] but the lack of a unified and quantitative treatment of the electronic structure of the CTTS state remained. The reader is referred to Blandamer and Fox's review for comparison of these models and their relative merits and failures.[1]

There have been two recent theoretical studies of the halide CTTS phenomena that require special mention.[12,19-25] Sheu and Rossky, using a sophisticated methodology for coupling the evolution of the solvent molecules to electronic changes in the solute, examined the iodide CTTS system in detail.[12,19-21]. Borgis and Staib explored the chloride CTTS system with a

similar approach.[22-25] Both groups use mixed quantum/classical simulations that include non-adiabatic transitions between electronic states so that the dynamical evolution of the excess electron could be followed subsequent to preparation of the non-equilibrium initial state. One of the earlier results from Sheu and Rossky's calculations was a simulation of the CTTS absorption band,[21] however no attempt was made to get quantitative agreement for the band position with experiment. The likely source of the discrepancy with experiment is the limited treatment of the electronic structure of the iodide ion (the use of a one electron model). It would be extremely useful to make accurate estimates of the CTTS binding energies and vertical transition energies so the spectra of various inorganic anions in polar solvents could be predicted. Only a handful of common anions have assigned CTTS transitions in solution,[1,18] although these types of bands should be relatively pervasive for anions in polar solvents.

Another new twist in the story of the halide CTTS system is the recent advent of cluster experiments in the gas phase addressing the spectroscopy[26] and dynamics[27] of CTTS "precursor" states in hydrated iodide. Prompted by the cluster work, several ab initio calculations finding solvent stabilized excited states of anions have appeared within the last two years.[28-33] As the clusters possess neither complete confinement nor an extended polarization of the environment it seems reasonable to re-examine the electronic structure of the CTTS state in bulk solution and further explore whether an ab initio description can be found for the latter. In particular, it is interesting to explore the dominant ingredients that lead to solvent-induced electron binding in the vertical CTTS state and ask whether there is a useful connection between the electronic structure of halide excited states in water clusters with that in aqueous solution. Rather simple questions may be posed: what is it about the solvation environment that leads to the appearance of CTTS states and how many solvent molecules are required?

It is perhaps important in this regard to distinguish two classes of hydrated anion structures in clusters. The *surface* isomers have the halide ion asymmetrically solvated.[34] For these clusters, excited states exist because the excess electron is bound by the net dipole moment of the water network. These excited states are akin to the dipole-bound ground states of excess electron in water clusters.[35-37] On the other hand, *solvated* isomers, which can also be termed interior or embedded structures, correspond to configurations where the anion is largely encapsulated by water molecules. Because of this more symmetric solvation, the net dipole of the water framework is smaller than for surface isomers. It is intuitive to focus on the solvated cluster configurations of hydrated iodide in a first attempt to represent the bulk environment.[38] However, the solvated geometries do not in general correspond to the lowest energy isomer of the ground state anion (*e.g.,* in aqueous chloride, bromide, or iodide clusters).[39] Consequently, except in the recent stimulating paper by Chen and Sheu,[30,31] they have rarely been examined in cluster calculations for their excited state spectrum. As we will emphasize, the solvated structures typically have very small electron binding energies for the excited states of the anion. There is a tendency by many researchers to look at solvation phenomena by a "building-up" approach from clusters assuming that the first solvation layer captures a large part of the condensed phase effect, and implying that small corrections due to long-range polarization can be applied to yield the bulk result. We will examine this building-up approach in detail for the CTTS phenomena and find that one has to be extremely careful in generalizing the cluster results even qualitatively. This can be contrasted to the tendency for surface solvation of polarizable anions such as iodide, which, although much stronger in clusters, is one property that has been predicted to carry over to the bulk - there is an excess of iodide in the interfacial layer of aqueous iodide solutions.[40,41]

5

Our studies are therefore motivated by an interest in finding accurate methods for computing the vertical excitation energies of anions in bulk water[42] by ab initio methods, and connecting how the energy of the lowest CTTS state transforms from cluster to bulk. We focus here on the prototype charge-transfer-to-solvent system, $\bar{I}(aq)$. As a secondary goal, we are interested in understanding the nature of the CTTS absorption spectrum, its width and oscillator strength. In this paper, we describe an ab initio model that is predictive for the energies of CTTS states and is readily applicable to a range of molecular anions in water. We stress that our approach is complementary to that of the non-adiabatic quantum dynamics simulations,[12,19-25] which allows for simulation of the full absorption lineshape as well as prediction of the detachment dynamics subsequent to CTTS excitation. However, the price for following the trajectory of the electron in time is to sacrifice a full description of the electronic structure of the solute. Our strategy in contrast is to use an ab initio treatment of the solute and first solvent shell while treating more distant waters as point charges, however, we will be limited to consider only time snapshots that simulate the vertical transition initiated by the photon. This allows an excellent description of the excited state eigenstates at time zero as well as an estimate of the inhomogeneous contribution to absorption lineshape. The shape of the initial wavefunction is in fact rather suggestive of the subsequent dynamics. In a later paper, we will examine the higher lying CTTS states and the forces on the solvent molecules in the lowest CTTS state at time zero. This latter information can be used to further quantify the CTTS lineshape, predict the Raman active modes[32] and point to the dominant motions at earliest times that lead to electron separation. We show that accounting for the long-range polarization field of the solvent using point charges at the positions of the solvent atoms, even including the first solvent shell merely as point charges, is sufficient to reproduce the CTTS energy and wavefunction of iodide in

6

water. Finally, we emphasize the importance of solvent fluctuations in the room temperature description of the aqueous solution.

2. Computational Methodology

The following computational strategy has been adopted for calculating CTTS states of iodide in water clusters. The singlet CTTS states have the same spin multiplicity and, in general, the same symmetry as the ground state of the system. Therefore, a rigorous quantum chemical procedure for their description should be based on a multi-configurational description. Such an approach, namely a complete active space multi-configurational method with a second order perturbation correction (CASPT2) has been recently adopted by Vila and Jordan for the description of the $I^-(H_2O)_4$ cluster.[33] Unfortunately, CASPT2 calculations are highly demanding computationally and become impractical for larger system, which are in focus of the present study. In contrast, the lowest triplet CTTS state may be readily computed by methods based on the single reference Hartree-Fock (HF) approximation.

For bare iodide in the gas phase, the lowest triplet, as well as the first excited singlet states are unbound. Therefore, if a bound triplet or excited singlet state can be found in a cluster, it is necessarily stabilized by the water environment. Furthermore, an electron promoted to an orbital corresponding to a CTTS state is only very weakly associated with the nuclear core of iodine, therefore, the singlet-triplet splitting is small. This can be verified by reference to energies calculated for the $I^-(H_2O)_4$ cluster by Vila and Jordan using the CASPT2 method, or, less rigorously, by either inspecting configuration interaction with single excitation (CIS) energies or comparing our triplets with energies obtained by Sheu *et al.* for the CTTS singlet states using single-reference wavefunctions (section 3.A below). In summary, the present approach is based on the possibility to employ low-cost single-reference methods to calculate the

lowest triplet CTTS state and, at the same time, learn quantitatively about the corresponding spectrally bright lowest singlet CTTS state.

For the evaluation of the lowest triplet CTTS state in iodide-water clusters, we have employed the Moller-Plesset second order perturbation theory (MP2). While a modest level of treatment of correlation is sufficient in the present systems where electrostatic interactions dominate, a great care has to be devoted to the choice of a proper and sufficiently flexible basis set. In particular, inclusion of very diffuse basis functions is already crucial for reproducing ground state properties (such as iodide ionization potential and polarizability), this issue being even more important for an adequate description of the more diffuse CTTS states. As in the previous study of Chen *et al.*, we have employed the diffuse functions augmented triple-zeta plus double polarization correlation-consistent (d-aug-cc-pVTZ) basis set for all the 18 valence electrons of iodide.[30,43] This basis set has been further augmented by a very diffuse *sp* even-tempered set[30] with six exponents forming a geometric series with a factor of five and lowest exponent of 2.35×10^{-6} au^{-2}. We have verified that an additional extension by an analogous diffuse set of *d*-functions changes only marginally (by less than 0.1 eV) the electron binding in the lowest triplet CTTS state. The iodine core electrons have been treated using a relativistic "small core" pseudopotential,[44] modified by Combariza *et al.* in order to reproduce the gas phase ionization potential of iodide.[43,45] This comparison assumes the lower $^2P_{3/2}$ spin orbit state of neutral iodine; thus, all results in this paper should likewise be referenced to the lower neutral spin-orbit component in experimental data. Also consistent with Chen and Sheu, a standard 6-31$_{++}$G* basis set has been employed for the water molecules.[30]

For the study of CTTS states of iodide in bulk liquid water, a modified strategy has been employed. As a first step, a classical molecular dynamics (MD) simulation has been performed.

A single iodide ion has been surrounded by 864 water molecules in a box of roughly $30 \times 30 \times$ 30 Å and periodic boundary conditions have been applied. In addition to bulk water, we have also simulated a water slab possessing two air-water interfaces by extending one of the box dimensions to 100 Å. Simulations have been performed at 300 K at constant pressure for the bulk, or constant volume for the water slab. A polarizable SPC/POL model of water and a polarizable model for iodide have been employed.[46-49] The polarizability used for I is 6.9 Å^3.[48,49] We note that this value, which takes into account the solvent induced decrease of polarizability, differs from the gas phase value employed Sheu.[21] An interaction cutoff of 12 Å has been used and long-range Coulomb interactions have been summed up via the particle mesh Ewald algorithm.[50] In principle, one could also apply a different MD approach to embedding an ion in bulk water such as the spherical model of Warshel *et al.,*[51] however, that would not allow to simulate the ion at the vapor-liquid interface. Simulations have been run for 500 ps after 250 ps of equilibration. 500 geometries corresponding to snapshots along the MD trajectory separated by 1 ps have been saved for further calculations.

In a second step, we have performed MP2 calculations for the ground state and the lowest triplet CTTS state of iodide and for the ground neutral iodine for 500 geometries along the classical MD trajectory in water. This ensures fair statistics for the vertical binding and transition energies. To make the calculations computationally feasible, we have replaced all 864 water molecules by point charges of -0.82 for oxygen and 0.41 for hydrogen.[52] In order to verify this approach, we have also performed, for selected geometries, calculations with water molecules in the first solvation shell around iodide treated explicitly, the remaining waters replaced by the above point charges. For the latter calculations, a cutoff of 4.4 Å has been employed to define the first solvation shell. These more complete and systematic calculations at representative snapshots

allow evaluation of the major factors influencing the CTTS stabilization in bulk solvent compared to small clusters. For each of the 500 snapshots, we have actually evaluated the energies of all the three subcomponents of the lowest triplet CTTS state (detached neutral) corresponding to electron promotion (removal) from one of the three valence *p*-orbitals of iodide. In addition, we have also performed CIS calculations, in order to obtain an estimate of the energy manifold of the low-lying CTTS states and of the corresponding singlet-triplet splittings. We carried through the basis set defined above for the cluster calculations to these "bulk" calculations. These calculations allow accurate estimates of the CTTS band position and inhomogeneous width as well as the energetic threshold for electron detachment into the gas phase.

All of the ab initio calculations have been performed using the Gaussian98 program.[53] The classical MD simulations have been carried out using the Amber6 program package.[54]

3. Results and Discussion
A. Gas phase clusters

Although the focus of the present work is in bulk electronic structure, we have found it useful to revisit some cluster calculations to establish our computational procedure. It is also illuminating to explore the relative sizes of the solvent induced binding of the excess electron in clusters as compared to the bulk. Table 1 summarizes our calculations for two cluster systems: a small one containing two solvent molecules and a larger one with six waters. We have started with the optimized geometries for iodide solvated by a water dimer and for iodide placed in the interior of a water hexamer.[43] The latter is not the lowest energetic isomer, however, it is the smallest cluster that allows for modeling iodide embedded in a solvent shell.[30] Then, we have computed the vertical electron detachment energy (VDE) from the ground state anion; this is

10

equivalent to the total energy difference between anion and the corresponding neutral cluster at the equilibrium geometry of the anion (often called the vertical electron binding energy (VBE)). These calculations reproduce previous work.[30,43] Then at the ground state anion geometry, we have computed the lowest triplet wavefunction and energy. We have been able to locate bound triplets for both the dimer and interior hexamer systems. The vertical electron binding energy for the promoted electron and vertical transition energy from ground to triplet state are shown in Table 1. The VBE's are indeed small and the triplet state is rather fragile.

To make direct contact with experiment and to evaluate whether our approach focusing on triplets will be fruitful, we compare the triplet transition energies to those for the first excited singlet. Chen and Sheu converged the lowest excited singlet state as a single reference state using a neutral iodine trial wavefunction. Strictly speaking, this Hartree-Fock excited state solution is not variational, nor is the MP2 correction valid for an unstable wavefunction. In contrast, the lowest triplet state is rigorously computed by single reference unrestricted Hartree-Fock method. Moreover, as the promoted electron is only weakly associated with the nuclear core, the singlet-triplet splitting is expected to be small and the highest occupied molecular orbital (HOMO) in the triplet and singlet should be very similar. For the purpose of comparison, we were able to reproduce the singlet excited binding energy for the dimer using Chen and Sheu's prescription and include all the relevant singlet CTTS data from their paper in Table 1.[30] The singlet-triplet splittings are confirmed to be quite small. For the dimer, the difference between the triplet and excited singlet is negligible (~ 3 meV); for the hexamer, the splitting has increased to 85 meV. In Fig. 1, we show the shape of the triplet HOMO for the interior hexamer; this compares very favorably with that of the singlet state, as shown in Fig. 2(c) of ref. [30]. Notice

that the promoted electron occupies space in the void but is in intimate contact with a number of (electron deficient) hydrogens.

We have further employed the configuration interaction singles (CIS) method to examine the CTTS manifold of excited states. With a diffuse enough basis, the CIS method simulates the detachment continuum as a series of equal transition energy promotions with effectively zero oscillator strength and bound states below the continuum appear as discrete excitations. The CIS method captures two excited states below the detachment continuum for the dimer and four for the interior hexamer, although we can see that there is a systematic overestimation of the transition energy (by ~ 0.3 – 0.4 eV) when comparing to the MP2 triplet excitation energies. In comparison, CIS calculation for the bare ion yields a series of continuum levels at 3.458 eV (again about 0.4 eV too high compared to the MP2 value). The early calculations of Combariza et al. were unable to find vertically bound excited states in water clusters[43] leading to a speculation that dipole bound excited states were beyond the reach of the CIS method.[30] In contrast, our results clearly reveal that with an adequate basis (i.e. with an appropriate choice of diffuse basis functions) CIS yields satisfactory results. Overall, our comparison shows that the excited state singlet and triplet are quite similar and the energetic splitting is small and quantifiable using the CIS energies. This comparison confirms that our triplet approach provides an acceptable strategy for estimating the CTTS transition energies and wavefunctions.

While the cluster results help to shape the methodology and are interesting in their own right, they are but a small step towards an accurate description of the CTTS state in bulk water. Although the vertical binding energy for all anion states grows rapidly upon increasing the number of solvent molecules (see Table 1), there is another 2 eV of binding to be recovered in the ground state until we reach the vertical detachment threshold for the bulk.[55,56] Chen and Sheu

comment that the CTTS transition energy for the interior hexamer is not far from the value observed in the bulk.[30] Likewise, Figure 2 in Serxner's experimental spectroscopy paper of hydrated iodide clusters implies there is a only a relatively small extrapolation in the transition energy from the CTTS precursor state with two to four waters to reach the bulk transition energy.[26] However, these observations overlook the fact that the electron binding for both ground and excited states in the bulk are both well over 1 eV larger than observed in the hexamer.[55] We will argue that this change in total electron binding leads to a qualitatively different form of the CTTS wavefunction, and thus the correct bulk description is not possible without including the effect of the extended environment into the calculation.

B. Reaction Field

The simplest effective treatment for taking into account the extended nature of the solvent in the bulk is to encapsulate the ion or ionic cluster in a dielectric continuum.[57] The polarizable continuum method has been extensively used in calculating the effect of solvation on equilibrium properties. It is interesting to consider if the polarization induced in a continuum solvent field is able to capture the time-zero solvent stabilization of the CTTS state in the spirit of the diffuse model of Franck and Platzmann and Treinin.[4,13] A similar approach has been attempted by Christiansen *et al.* to compute ab initio the absorption spectrum of liquid water.[58] To properly calculate the vertical excitation energy, the polarization of the dielectric needs to be broken into the instantaneously responding electronic contribution of the solvent molecule electron clouds and the slowly responding polarization due to the positions of the solvent nuclei.[59] The latter should be frozen to compute the vertical transition energy. Methods have been constructed to compute this non-equilibrium reaction field response,[60,61] but they are not available within standard electronic structure packages. We therefore made only a trial foray into exploring a continuum treatment. We used the Tomasi polarizable continuum model

13

(PCM),[57] as implemented in Gaussian98, around bare iodide and around the interior $I^-(H_2O)_6$ structure to see how much stabilization results for equilibrium polarization. Both representations show substantial additional triplet binding (> 1 eV). We prefer the calculation with the first water shell explicitly included as this freezes the nuclear polarization at least in the first shell and avoids the possibility of a substantial fraction of the triplet HOMO wavefunction spilling outside the PCM cavity. Table 2 also includes a result for a self-consistent reaction field around iodide embedded inside a first solvent shell captured from the MD run (see below). The binding energy of the CTTS triplet state at the MP2 level is again increased by ~ 1 eV compared to stabilization provided by the first shell only.

It is often stated in the literature that much of the condensed phase effect on solute electronic structure may be reproduced by using a gas phase cluster as the first solvation shell in conjunction with a continuum model for the long range solvent effects.[58] We see that indeed a substantial part of the electron binding for anion ground and triplet states derive from other long range polarization, and about 80% of this effect is captured by the reaction field approach. Note that our test result, obtained using an equilibrium continuum model, should overestimate the electron binding energy since it includes the additional stabilization due to relaxation of the nuclear polarization after vertical excitation. Moreover, we will see that, in comparison to the use of a more textured electrostatic potential for the extended solvent environment, the cluster plus reaction field model misses two key features. Namely, it fails to get the correct shape of the excited state wavefunction and omits the substantial variation in the binding energy due to solvent fluctuations.

14

C. Classical equilibrium MD results

    To include the disorder intrinsic to liquid water, we turn to the use of equilibrium

molecular dynamics simulations to sample the variety of solvent configurations around the

(ground state) anion that exist for a room temperature solution. We note that due to thermal

disorder, even the first solvent shell in these configurations is unlikely to be as favorable for

stabilizing the halide anion as the low temperature cluster configurations examined above.

Further, due to the strong solute-solvent coupling, we expect a large dispersion in the calculated

vertical electron binding energies from this ensemble of configurations. First, let us examine the

equilibrium properties predicted by the classical molecular dynamics.

    From a 500 ps equilibrium simulation, the iodide – oxygen radial distribution function,

$g_{I-O}(r)$ is computed and shown in Fig. 2. The simulated g(r) peaks at 3.55 Å and has a minimum

around 4.3 – 4.4 Å, both in good agreement with experiment,[62] and the g(r) is in close agreement

with that reported by Dang.[48] Iodide, as a particularly large and soft anion, is not expected to

strongly order the solvent and this is evidenced by the weak second and third recurrence in the

simulated g(r); these are even weaker in the experimental X-ray determinations.[62] The computed

average number of waters in the first solvent shell is 8.5, using 4.4 Å as the cutoff for the I^- - O

distance, in good agreement with experiment.[62]

D. Ab initio calculations at instantaneous molecular dynamics configurations.

    Our strategy is to find the vertical energy separations between the anion ground, CTTS

and neutral states by ab initio methods for an ensemble of solvent configurations in the MD run.

First, for a small set of solvent configurations from the equilibrium MD run, we made a few tests

to evaluate the approach of treating the solvent by distributed charges. This also allowed for

decomposing the excess electron binding energy for each of the anion states into that arising

from the first water shell and that from the extended orientational polarization of the solvent.

Initially, to make a direct comparison with the interior clusters, we take only the first solvent shell from a MD snapshot. Table 2 compares the ground and triplet state binding energies for a single snapshot when the first shell solvent molecules are treated explicitly in a full ab initio calculation (comparable to the cluster calculations above) and when the solvent shell appears in the ab initio calculation only through its atomically resolved electrostatic field around the anion. Interestingly the two approaches give quite similar results and it is clear that although a triplet state is bound in both approaches, the vertical binding energy is negligibly small, and smaller even than that for the interior hexamer cluster. We emphasize that the geometry of the first shell from the room temperature snapshot is quite different from the minimum energy geometry expected for that size cluster. This effect is reflected in Table 2: the ground state binding energy, which mostly reflects the strength of the anion solvation, is only comparable to the interior hexamer cluster, despite the larger number of waters (eight) in the snapshot calculation.

Next, we include the effect of all 864 water molecules from the molecular dynamics simulation. The distant waters are included as distributed fractional point charges explicitly on oxygens and hydrogens to capture the extended electrostatic polarization of the environment. As before, the binding energies are compared for two models: when the first solvent shell is treated fully ab initio and when even this shell is treated as point charges. We note that the former model is already relatively expensive for a statistically relevant number of MD geometries. An even more sophisticated approach based on treating two full solvent shells quantum mechanically with the remainder as point charges would require > 800 basis functions and is therefore computationally rather prohibitive. However, the results in Table 2 show that the explicit inclusion of all electrons on the first water shell, so as to include the effect of Pauli

repulsion between the diffuse excess iodide electron and electrons on the neighboring solvents (and to include the electronic polarization of the electrons in the first shell waters), seems relatively unimportant. The triplet binding energy calculated by the two approaches differs only by 8%. This same comparison has been made at five additional snapshots; these results are given in greater detail in Table 3.

The most immediate message from Table 2 is that the inclusion of the long range electrostatic field beyond the first hydration shell leads to an additional 2 eV stabilization for the ground anion state relative to the neutral. Likewise, virtually all the triplet state binding results from the long-range pre-existing (*i.e.,* caused by the ground state anion) nuclear polarization of the solvent. Inspection of Table 2 and 3 indicates that the point charge treatment of all solvent molecules turns out to be a surprisingly accurate approximation, as judged by comparison to experimental values for both the anion ground and CTTS binding energy, and the relatively small changes in these energies when treating the first shell quantum mechanically. Note also, that a Hartee-Fock treatment of the iodide already captures a large part of the binding energies but it consistently underestimates it by ~ 0.5 eV compared to the MP2 result for both cluster and bulk systems. We conclude that the distributed charges model for all solvent molecules for recovering the instantaneous nuclear polarization of the solvent is accurate and captures most of the essential physics. Careful comparison of the ensemble average values with experiment is made in Section 4.

Single point CIS calculations (Table 3) at the geometries of each of the representative snapshots point to an approximately constant splitting between the lowest triplet and singlet excitation of 0.3-0.4 eV. We note that compared to clusters, the singlet-triplet splitting is increased as expected for a more strongly bound CTTS electron. However, it is still small

enough so that the triplet calculations continue to provide a good basic description of the electronic character of the CTTS states in the bulk and, since they are reliably converged, they allow for extensive sampling of geometries as shown below. Results from the CIS calculations are discussed in further detail in section 3.G.

Let us turn to the shape of the electronic wavefunction predicted from these calculations for the triplet CTTS state. The promoted CTTS electron occupies an orbital (Fig. 3) with a highly asymmetric shape. There is a radial node in the wavefunction. The outer lobe (blue mesh in Fig. 3) is extremely diffuse, centered at a radius of 3 Å, and extending to ~ 4.5 Å from the iodine center while the inner lobe resides close in to the iodine. The volume of the outer lobe is ~ 80 Å^3 for a limiting isodensity value of 0.025. Inspection of the promoted electron orbital in each of six snapshots detailed in Table 3 indicates that the electron density is channeled into void regions in the *first solvent shell*, and thus the shape of this orbital is defined by the asymmetry of the water environment around the iodide at the instant of photoexcitation. Consistent with the rather small differences in the binding energies, there is only a very small change in the shape of the triplet HOMO when comparing with computations using a less rigorous, purely electrostatic treatment of the first solvent shell. This suggests that electron density is not artificially trapped at the hydrogen atoms when the first shell is included only by point charges. Such a localization of the electron near hydrogens would result in a prohibitively large kinetic energy penalty; therefore, it does not occur even when the hydrogens are modeled simply as positive fractional charges.

E. Iodide in bulk water – ensemble of vertical energies
The results in the previous section give us confidence that the relatively simple and computationally cheap model where the solvent is merely treated by an extended, but atomically-resolved, charge distribution captures the essential physics of the phenomenon. However, it is

immediately apparent from Table 3 that there are relatively large variations in the vertical energies as the solvent samples different configurations about the anion. Therefore, we accumulated greater statistics using the distributed charges electronic structure model for an ensemble of solvent geometries sampled over the room temperature MD run.

Sheu and Rossky's results emphasized the lowest CTTS wavefunctions as having considerable *d* character at the instant of excitation.[21] Supplementing our basis with an identical geometric series of diffuse d-functions as the *sp*-series used (see section 2) leads to only a very slight (< 0.1 eV) stabilization of both the ground and triplet states in each of the snapshots of Table 3. However, as there is a slight change in the shape of the promoted electron orbital and as we wish to compare our CTTS wavefunction to ref. [21] we retained the *d*-function supplemented basis in our final production run. Thus, we computed the vertical ground state and triplet binding energies for bulk I$^-$ at every 1 ps of the 500 ps run.

A summary of the resulting statistics from this run is given in the upper part of Table 4. The average electron binding energies are comparable to the "representative snapshot" shown in Fig. 3 and detailed in Table 2; the average triplet state binding is substantially larger than for the gas phase clusters. In Fig. 4, we have plotted a histogram of the energies of anion ground and lowest triplet CTTS state relative to the vertically detached iodine. There is considerable spread in the vertical detachment energy at different solvent configurations and this physical distribution is more significant than the numerical inaccuracies resulting from choice of basis set, solvation shell model or singlet-triplet splittings we have concerned ourselves with above. As the fluctuations in ground and triplet binding energies are correlated, the excitation energy standard deviation is smaller but still is ~ 0.2 eV. Thus, solvent fluctuations are highly significant in a description of the bulk electronic structure and entirely omitted from traditional models [4,13,15,16,63]

19

or from a cluster-embedded-in-continuum approach.[61] The spread in the vertical excitation energy will be discussed in more detail when we consider the CTTS lineshape.

F. Iodide at the air-water interface:

It has been shown recently that iodide in water exhibits surfactant activity, *i.e.,* its concentration at the air-water interface is enhanced with respect to the corresponding bulk value.[40,41] Various recent experiments have selectively probed iodide at the liquid-vapor interface.[56,64] From this point of view, it is of considerable interest to investigate the character of the CTTS state for surface solvated iodide. For this purpose we have performed MD simulations of a water slab with the anion initially place at the vapor-water interface (see inset of Fig. 5 and ref. [65] for details). Due to the preference for surface solvation, iodide actually remains in the interfacial region for the duration of the MD simulation without imposing any additional constraints to its motion.

The results for the slab simulation, concerning binding energies of the ground and lowest triplet CTTS states of iodide along a 500 ps trajectory are summarized in the bottom of Table 4 and a typical wavefunction of the CTTS electron is depicted in Fig. 5. The most important conclusion is that the character of the CTTS state, as well as of the ground state, does not depend qualitatively on the (interfacial or interior) solvation site. The electron binding is similar, but slightly greater, for iodide at the interface compared to that buried in the interior. This can be rationalized as follows. First, the long-range disorder in a liquid smears out to a large extent the difference between various solvation sites. Second, a surface solvated iodide loses binding to one or two waters in the first solvation shell which is, however, compensated by the rise of induction energy due to an asymmetric solvation of a polarizable solute in a polar solvent.[40] As a result, on average iodide acquires 0.1 eV of additional binding at the interface compared to the bulk. In the

CTTS state this difference increases to 0.26 eV. This can be attributed to the increase of iodide polarizability upon excitation to a more diffuse (and therefore more polarizable) CTTS state.

Clearly, the behavior of iodide in the bulk differs from that in finite size clusters, where the effect of surface vs. interior solvation on the binding of a polarizable anion is much more pronounced.[65] For example, for surface iodide in water clusters, the CTTS precursor state corresponds to a dipole-bound diffuse electron outside the cluster, while at the bulk interface the CTTS electron is located in a cavity within the solvent (see Fig. 5) rather than pointing into the low density phase. Finally, we note that our findings concerning surface vs. bulk solvation of iodide are in accord with a recent study of the solvation of chloride anion in various aqueous environments.[65]

G. Symmetry breaking of the occupied p-orbitals

So far, we have concentrated on the lowest single excitation into the triplet and neutral manifold, however there are three low-lying one-electron excitations possible that derive from the three valence p-orbitals of I^-. Due to the asymmetry of the solvent, the p-orbitals are no longer degenerate. Vertical CIS single point calculations at several solvent snapshots clearly point to three excitations in the singlet manifold with significant oscillator strength, whose excitation energies are closely clustered (within 0.25 eV); likewise, there are three excitations in the triplet manifold with similar splittings. The orbital to which the electron is promoted in each of the three low-lying excitations has primarily s and p character. For both multiplicities, there is a ~ 0.5 – 0.7 eV gap until the next higher states in the CIS excited state spectrum. Promotions to orbitals with a substantial d character occur in our calculations at energies much closer to the continuum. The CIS calculation also provides estimates for the singlet transition oscillator strengths. For each singlet sub-band within the first CTTS set of states, the oscillator strength is

~ 0.15, giving a combined strength for the lowest band of 0.45. It is interesting to note that if only the first solvent shell is included in the calculation, then the CTTS band has very little oscillator strength. This highlights the importance of the long-range polarization in reproducing both the position and intensity of the CTTS band.

In order to get an estimate for the relative broadening of the CTTS band by the solvent-induced breaking of p-orbital degeneracy as compared to the inhomogeneous broadening due to fluctuations in the surrounding solvent configuration, each of the three subcomponents of the triplet and neutral manifold of states corresponding to promoting the different iodide p-electrons were computed. Fig. 4 shows only the energy difference between the lowest components of each manifold. The spectrum of vertical excitation energies from the anion ground state to the full CTTS triplet band, and its breakdown into sub-bands is represented in Fig. 6. The average transition energies for the three sub-bands are 5.53, 5.65 and 5.78 eV, and the full width at half maximum is 0.49 eV. The singlet CTTS spectral band would be expected to be similarly constituted but shifted to higher energy by ~0.4 eV, based on the CIS singlet-triplet separation (Table 4).

4. Comparison with experiment

Our bulk calculations predict two vertical energy gaps that may be compared with experiment. An estimate of the vertical electron binding from the ground state of aqueous iodide is given by the photoelectron emission threshold. Watanabe and coworkers report a threshold energy of 7.02 eV.[55,56] At the photoelectron threshold, the optical excitation accesses the transitions from the least favorably solvated iodide anions and from the highest lying p-orbital. Strictly, the experimental values should be compared with the low binding energy wing of Fig. 4 and our model appears to be slightly underestimating the threshold. There is obviously better

agreement between experiment and the *average* binding energy from the distributed charges simulation (7.05 eV; Table 4). Treating the first solvent shell inside the ab initio calculation would increase the binding energy on average by ~ 0.2 eV (Table 3). Further, although the experimental values are taken by Watanabe and coworkers to infer the bulk vertical ionization energy, the experiments are actually only sensitive to the *surface* of the aqueous solution, [55,56] and thus should be compared to interfacial simulations. The results in section 3.F suggest that surface iodide is bound ~ 0.1 eV more strongly compared to an ion truly in the bulk. This further reduces the discrepancy between experiment and simulation. Overall, we consider the agreement with the photoemission experiments to be good.

To consider the performance of the model for anion excited states, we can compare to the spectral band for the lowest I^- CTTS transition in water at room temperature. The experimental band is centered at 5.5 eV with a full width at half maximum (FWHM) of 0.6 eV; this band corresponds to the low energy band of a spin-orbit doublet. Fig. 6 shows the histogram of ground to triplet transition energies – when all three p sub-bands are considered, the central transition energy is 5.6 eV. A Gaussian gives a good fit to the histogram and has a FWHM of 0.5 eV. However, it is not the triplet manifold that carries the oscillator strength for transitions from the ground state. Using the CIS CTTS singlet-triplet splitting as a guide, we would predict an absorption spectrum similar to the histogram shown in Fig. 6, displaced to higher energy by 0.4 eV. Therefore, the distributed charge model would put the CTTS band center at 5.9 eV. Once again, we consider this level of agreement with experiment quite promising, particularly considering the first principles nature of our quantum chemical calculations. The good agreement in both the ground-CTTS energy gap and the ground state anion vertical detachment energy with experiment means that we are quantitatively reproducing the excited state vertical

binding energy. In order to further elaborate on the character of the manifold of the excited states one would have to include explicitly the effect of the spin-orbit interactions. A promising strategy would be, e.g., to treat the spin-orbit couplings starting from a diatomics-in-molecules approach[66,67] for the iodine atom-electron pair.

The average oscillator strength (~0.45) predicted by the CIS calculations for the combined set of three lowest singlet excitations is in good agreement with experiment. The overall oscillator strength for the spin-orbit split doublet in the experimental spectrum is quoted by Jortner[2] as 0.47. This should be compared to a total possible oscillator strength of 6 for transitions promoting any of the six 5p electrons.[2,21] The good agreement in the calculated and experimental band oscillator strength indicates that we have an accurate description of the excited state wavefunction and supports the notion that a single excitation description for the excited state is adequate.

The experimental linewidth of the CTTS transition is due to three major sources. (i) Inhomogeneous broadening due to the distribution of instantaneous configurations of the water network. We have seen that this leads to a wide distribution of vertical transition energies (Fig. 4). (ii) Substructure in the overall band due to different electronic components. These first two sources combined lead to ~ 0.5 eV full width at half maximum in our simulations. (iii) Homogeneous broadening due to reorganization of the bulk water in response to the electronic excitation. A large part of this effect is due to movement of waters in the first shell.[68] This is not included in our time zero calculations.

In the series of effective one electron model simulations of the hydrated electron and aqueous I[-], all three contributions are included and in each case electronic sub-structure is important in determining the lineshape.[17,21] However, in Sheu and Rossky's simulation of the I[-]

24

CTTS band, six different sub-states contribute with almost equal intensity to the spectral line with total bandwidth of 0.8 eV, with approx. 0.4 eV width for each sub-band.[69] The six sub-bands were assigned to promotion of the single electron from a single p-state into one of six *s* and *d* character states.[21] Our CIS calculations clearly show a group of only three excitations arising from promotion of one of three near-degenerate filled p-orbitals to a single CTTS orbital. The CTTS orbital is primarily a mixture of *s* and *p* character basis functions. We return to this discrepancy with the one electron model of Sheu and Rossky below.

Unlike the solvated electron lineshape, the observed iodide CTTS lineshape is Gaussian. The solvated electron band has long been known to have a complex lineshape that can be approximated by a Gaussian function on the red side of the peak and a Lorentzian to the blue.[70] As detailed above, the prevailing explanation for the solvated electron lineshape has come from quantum/classical simulations with three underlying *s-p* transitions split by the solvent asymmetry and a tail explained by the onset of the liquid conduction band.[17] This picture is supported by pump-probe experiments in the band center.[71,72] Recently, it has been proposed based on photon echo experiments, that the lineshape for the solvated electron can be described entirely by homogeneous broadening and the lineshape is a generalized Lorentzian, which deviates from a standard Lorentzian form when the central frequency is on the order of the reciprocal dephasing time.[73] The iodide CTTS transition is often compared to the solvated electron absorption band, but with respect to the lineshape they are distinct – if the CTTS line were to be purely homogeneously broadened with a comparable 1 – 2 fs dephasing time claimed for the solvated electron,[73] the line would appear to be standard Lorentzian due to the higher transition frequency. As the experimental line is Gaussian, this would seem to support

inhomogeneous broadening such as that described in our model. This notion is confirmed by very recent hole-burning experiments on the related Na⁻ CTTS system.[74]

5. Conclusions

Shape of the CTTS electron orbital

The promoted electron in the CTTS state occupies available free space in the first solvent shell (Figure 3). This sensitively depends on the instantaneous solvent asymmetry and gives a clear explanation of why there is such strong solute-solvent coupling in the electronic transition. Thus the CTTS transition energy is rather sensitive to the environment temperature and pressure.[1] The range of the electron is not as great as the size of dipole bound excited states in clusters but it is somewhat larger (and the wavefunction is more non-spherical) than that of an equilibrated solvated electron.[17]

In all snapshots examined, the CTTS wavefunction always has node between iodide core and frontier lobe. It has the appearance of an orbital with a mixture of s and p character with a radial node reminiscent to that of a hydrogenic 2s wavefunction.[2] The observation of a radial node is consistent with the CTTS precursor wavefunction in surface clusters where it has been argued that this node leads to a repulsion between the separating electron and the iodine atom.[31] Breaking down the HOMO for the triplet anion at one test solvent configuration (that shown in Fig. 3) into its constituent basis functions indicates that the orbital is almost entirely described by valence *s (~30%),* diffuse *s (~50%)* and *p (17%)* type basis functions. The orbital has only 2% of a *d*-character even when a full set of diffuse *d* basis functions is included in the basis set. A similar result is found considering the transition density matrix to the CIS first excited singlet. This is in strong contrast to ~ 45 – 80 % *d*-character found by Sheu and Rossky in their lowest CTTS states, although the energetic ordering amongst the *s* and *d* states in their calculation

switches with the effective size of the iodine core.[12,21] As stated earlier, we find that CIS promotions into an orbitals with strong *d*-character have much higher energies in our calculation. We suggest that the neglect of all other valence shell electrons in the one electron model of Sheu and Rossky may lead to an artificial lowering of the energy of the *d* virtual orbitals.

Evolution of CTTS electron into solvated electron

The shape of the CTTS wavefunctions uncovered in this study is rather suggestive of the ensuing dynamics. Even on initial excitation, the strong asymmetry in the bulk environment has predisposed the electron to bud in a defined direction and is only in an ensemble average sense "still centered at the iodine atom".[1,4] Rearrangement of the adjacent waters, particularly translation of molecules away from where the excess electron is beginning to localize and concomitant reduction in the size of the electron cloud to match an equilibrated electron are the likely next steps. Other rearrangements, including waters pushing in toward the iodine atom from the opposite side and solvent reorientation, are expected. Analysis of the instantaneous first and second derivatives of the ab initio energies at MD snapshots with an explicit first solvent shell should be useful to quantify the dominant early nuclear motions.

Also important is the observation that the range of the CTTS electron, although diffuse with respect to the I atom, is restricted to the radius of the first solvent shell. Thus, it is reasonable to expect the fully relaxed electron to localize within the first solvent shell, in excellent agreement with the conclusion from experimental studies in our laboratory. We have found based on analysis of geminate recombination,[9] and solvation timescales[10] of the ejected electron from the iodide photodetachment system, that electrons localize close to the parent iodine in strong contrast to those liberated from the two-photon ionization of water or the one-photon detachment of $[Fe(CN)_6]^{4-}$. For H_2O ionization it is believed that the state accessed is

fairly delocalized (a mixture of molecular Rydberg and extended liquid conduction band character depending on the exact excitation energy [75,76]), consistent with observed ejection range. Static quenching experiments further distinguish the electron range of the optically pumped state;[76] recent experiments in our lab reinforce that the iodide CTTS wavefunction is not highly extended, [77] as compared to 2 photon excited H_2O or 1 photon excited $[Fe(CN)_6]^{4-}$.[76]

Ingredients of the CTTS binding

The binding in the cluster is a rather small part of the overall binding in the bulk. This is significant, and perhaps lost in concentrating on the transition energy [26,30]. The binding in the bulk appears to be determined by the long-range solvent polarization, so, in comparison to interior clusters, the qualitative description of the binding is changed when moving to the bulk.

Calculations based on MD with all solvents as point charges captures the vertical nuclear polarization but none of the electronic response of the solvents in computing the CTTS state energy. Given the success of the all charges model in reproducing the binding energies, we surmise that it is the nuclear polarization that is most important here. A number of recent ab initio calculations have characterized states as CTTS by evidence of electrons transferred onto specific water molecules.[28,29,32,33] Although we do see some excitations to unoccupied orbitals of individual water molecules when the first solvent shell is taken explicitly, these are rather delocalized over the first solvation shell. Since there is little difference between the explicit first shell and all charges models we will argue that charge transfer to an acceptor orbital localized on a particular solvent molecule or cluster is not important. For the same reason we conclude that the electronic polarization of the first solvent shell plays only a minor role. The essence of the presently used (electrostatically dominated) model is that the large nuclear polarization around the iodide ion at the instant of photon absorption dominates the CTTS state binding and the

effects of confinement and charge transfer to specific solvent molecules are relatively unimportant.

To further illustrate this point we have carried out an MD equilibrium simulation of an uncharged iodine atom in water, to remove the net solute-induced solvent nuclear polarization. In the same manner as earlier computations, we have then computed the electron binding for the various states of an iodide anion replacing the neutral iodine at solvent configurations along the trajectory. As expected, we have found a substantially smaller anion ground state binding. However, the average value (~2.6 eV) is even smaller than for gas-phase iodide. Moreover, the CTTS triplet state is only marginally bound at some instantaneous solvent configurations while at other snapshots the wavefunction fails to converge, indicating that it is very likely unbound. These observations are fully consistent with our description above.

5. Summary

We have demonstrated a method to reproduce the ground and excited state electronic structure of the iodide anion in water and presumably other simple anions in polar liquids. The method is computationally modest given the achieved accuracy and zeroes in on the importance of electrostatic interactions with an atomically resolved representation of the solvent in the accurate description of the CTTS phenomenon. We also find that role of solvent fluctuations is more important to the CTTS wavefunction and its energy than the fine detail of the ab initio method.

The availability of unoccupied space is crucial and the location and size of such voids in the close vicinity of the anion varies strongly with time. It is instructive to compare a surface hydrated iodide cluster whose CTTS precursor wavefunction pushes out into the vacuum, while for iodide at the bulk surface with longer range solvent polarization, the promoted electron

prefers to be buried in the solvent wherever there is a void in the first solvent shell. Pauli repulsion with the solvent electrons in the nearby shells makes only a small contribution to overall description. Likewise, the instantaneous electronic polarization of the solvent molecule electron distribution in response to iodide electron promotion is not very large. Apparently, on comparing our results with the one electron pseudopotential treatment used for iodide in the dynamical simulations,[21] a good description of the electron binding to the neutral iodine atom remains crucial even in the highly diffuse CTTS state. We therefore conclude that of the two early models,[4,13-15] the diffuse model emphasizing the long-range polarization is a better zero-order picture, but the neglect of the iodine core, fluctuations of the polarization field and creation of instantaneous asymmetry due to thermal disorder are serious limitations.

It is perhaps clear from this study that the cluster CTTS precursor excited in the spectroscopy experiments of Johnson[26] and whose femtosecond time dynamics is probed by Neumark[27] is a qualitatively different object than the CTTS state in solution. The excited state HOMO probed in these cluster experiments avoids the solvent and is highly extended compared to the bulk CTTS wavefunction, whereas the vertical electron binding is almost an order of magnitude stronger in extended systems.

Tables:

Table 1: Ab initio results for hydrated clusters of iodide containing two or six water molecules.

	HF	MP2	CIS	Experiment
Bare Iodide anion				
Ground state VDE[a]	2.420	3.033		3.0591[f]
Ground to Triplet exc.[b] (VBE)	2.420(0.000)	3.033(0.000)	3.458	
I⁻(H₂O)₂ [c]				
Ground state VDE	3.214	3.880		3.919[g]
Ground to Triplet exc. (VBE)	3.209(0.0049)	3.868(0.012)	4.238	
Ground to Singlet exc. (VBE)	3.210(0.0044)[d]	3.871(0.009)[d]	4.258	(0.03)[h]
V-shaped I⁻ (H₂O)₆ [c,e]				
Ground state VDE	4.131[d]	4.822[d]		5.1[g]
Ground to Triplet exc. (VBE)				
Ground to Singlet exc. (VBE)	4.003 (0.128)[d]	4.608 (0.214)[d]		(0.23)[j]
Interior I⁻ (H₂O)₆ [c]				
Ground state VDE	4.451	5.156		
Ground to Triplet exc. (VBE)	4.419 (0.032)	4.940 (0.217)	5.237	
Ground to Singlet exc. (VBE)	4.440(0.011)[d]	5.024(0.132)[d]	5.451	

[a]   Vertical detachment energies (VDE, eV) are from ground state anion to the lowest neutral state.

[b]   Vertical excitation energies (in eV) are from ground state anion to triplet and singlet excited states. Vertical electron binding energies (VBE) with respect to the lowest neutral state are shown in parenthesis.

[c]   All cluster structures are from ref. [43]

[d]   From ref. [30]

[e]   The lowest energy conformation of I⁻(H₂O)₆. ref. [43]

[f]   Ref. [45]

[g]   Ref. [38]

[h]   Ref. [26]

[j]   Ref. [27]

Table 2: The factors determining the vertical electron binding energy (VBE) for increasingly hydrated iodide. Various methods for incorporating the continuous solvent medium are compared.

System	Ground state V.B.E. (eV)	Triplet state V.B.E. (eV)
Bare I$^-$ ion	3.03	0
I$^-$ Clusters[a]		
Water Dimer	3.88	0.012
Water Hexamer Interior Cluster	5.16	0.22
Water Hexamer Interior in reaction field	6.23	1.31
Equilibrium solvent configuration[b] - only one shell of waters considered		
Solvent as charges	5.0	0.0002
Solvent explicitly QM	5.2	0.015
Equilibrium solvent snapshot[b] - Extended treatment of solvent		
Bare ion in reaction field	5.8	1.36
All solvents as charges	6.9	1.83
First shell QM, remainder reaction field	6.5	0.98
First shell QM, remainder as charges	7.1	1.69
Experiment	7.1[c]	(1.6)[d]

MP2 energies used throughout. All calculations use same basis (see text).

[a] Interior hexamer cluster also taken from [30]

[b] Based on single snapshot (50ps) from Table 3.

[c] Threshold photoemission from ref. [55]

[d] Based on ref. [55] and singlet CTTS peak position, ref. [1]

QM = quantum mechanical (ab initio)

Table 3: Iodide ion electronic properties evaluated at several instantaneous snapshots during the molecular dynamics trajectory. These snapshots are used to characterize the two approaches – explicit ab initio treatment of the water molecules in the first solvent shell with the remainder contributing as point charges and uniform treatment of all waters as charges.

	First shell (N waters) explicit, remainder charges			All 864 waters as charges		
	HF	MP2	CIS	HF	MP2	CIS
50ps	**N=8**					
Ground state VDE[a]	6.374	7.134		6.271	6.867	
CTTS Triplet[b]	4.981 (1.393)	5.441 (1.694)	5.779	4.636 (1.636)	5.041 (1.826)	5.286
CTTS Singlet[b]			6.148			5.637
100ps	**N=9**					
Ground state VDE	5.795	6.551		5.821	6.414	
CTTS Triplet	5.182 (0.613)	5.512 (1.039)	5.943	4.923 (0.898)	5.266 (1.148)	5.526
CTTS Singlet			6.291			5.873
150ps	**N=9**					
Ground state VDE	6.036	6.805		5.975	6.569	
CTTS Triplet	5.265 (0.772)	5.924 (0.881)	6.236	4.926 (1.049)	5.291 (1.278)	5.543
CTTS Singlet			6.433			5.872
200ps	**N=9**					
Ground state VDE	6.390	7.157		6.345	6.936	
CTTS Triplet	5.855 (0.535)	6.151 (1.006)	6.533	5.270 (1.075)	5.549 (1.388)	5.810
CTTS Singlet			6.892			6.212
250ps	**N=7**					
Ground state VDE	6.986	7.771		6.941	7.526	
CTTS Triplet	6.070 (0.916)	6.280 (1.491)	6.771	5.478 (1.463)	5.777 (1.749)	6.022
CTTS Singlet			7.095			6.409
300ps	**N=9**					
Ground state VDE	5.790	6.550		5.717	6.311	
CTTS Triplet	5.409 (0.381)	5.551 (1.000)	6.065	4.893 (0.824)	5.226 (1.086)	5.485
CTTS Singlet			6.438			5.852

[a]   VDE: vertical detachment energy from ground state anion to the lowest neutral state (in eV).

[b]   For the CTTS states, the vertical excitation energy from the ground state is shown, with the CTTS state vertical electron binding energy given in parenthesis. All energies in eV.

Table 4: Statistics from snapshots from a 500 ps dynamical run for I⁻ embedded in bulk water or sitting at an air-water interface. All waters are treated as point charges in ab initio computations. The basis includes a diffuse *d* set on iodide. Vertical binding and transition energy estimates are from MP2 energy differences or from CIS computation starting with ground state anion reference.

Iodide environment	Statistic	MP2 ground state VDE (eV)	MP2 triplet state VBE (eV)	MP2 ground → triplet energy (eV)	CIS ground → triplet (eV)	CIS ground → singlet (eV)
Bulk	Average	7.050	1.504	5.535	5.674	6.113
	Minimum	5.912	0.679	4.634	4.897	4.897
	Maximum	8.278	2.335	6.143	6.205	6.910
	Standard deviation	0.405	0.329	0.188	0.175	0.221
Interface	Average	7.176	1.760	5.416	5.567	5.970
	Min	6.209	1.110	4.788	4.988	5.202
	Max	8.389	2.614	5.973	6.067	6.618
	Standard deviation	0.346	0.267	0.176	0.168	0.197

Figure captions

Figure 1:   The HOMO of the lowest triplet state of the interior hexamer cluster. Each water molecule is shown as ball and stick and the iodine atom is at the center of the figure. The isodensity surface has a cutoff at 0.012. The state for which this orbital is the HOMO has been considered a precursor to the bulk CTTS state. The wavefunction is very similar to that depicted for the excited singlet in ref. [30].

Figure 2:   Simulated iodide-oxygen radial distribution function based on a 500 ps classical molecular dynamics run.

Figure 3:   The HOMO of the CTTS triplet state. Iodide in a box of 864 water molecules, captured at one instant in a molecular dynamics trajectory. The first solvent shell (defined by a cutoff in the I^--O radius at 4.4 Å) is shown with ball and sticks. All electrons on these water molecules are explicitly included in the ab initio calculation. The remaining waters (shown as sticks) are replaced by partial charges at the oxygen and hydrogen atoms in the calculation. The waters molecules outside the first shell are depth-cued: if the solvent is near the anion center it appears bright while those at large distances appear dark. The molecular orbital (blue mesh and white solid lobes are opposite sign wavefunction amplitude) is directed into a low-density section of the first solvent shell. There is a clear node in the one electron wavefunction between the iodine atom and the main amplitude lobe (in blue). (Inset) Iodide and the triplet HOMO with only the first solvent shell shown.

Figure 4:   Vertical electron binding energy from the anion ground (left panel) and first triplet state (right panel).   Statistics collected from solvent configuration snapshots over a 500 ps equilibrium molecular dynamics run.

Figure 5:   Typical shape of the HOMO of the triplet CTTS state for iodide at the air-water interface. Iodide (purple) is at the surface of a slab of 864 water molecules, captured at one instant of a molecular dynamics trajectory. The implementation of the slab configuration in the MD via a periodic box extended in one direction is schematically shown in the inset. All waters are replaced by partial charges at the positions of oxygen and hydrogen atoms in the ab initio calculation (see text). Notice that the molecular orbital (isosurface = 0.025, white and blue lobes are of opposite sign wavefunction amplitude) is directed toward the bulk and not into the vapor phase.

Figure 6:   The anion-triplet transition energy spectrum from same MD run as for Fig. 4. The lowest three components of the triplet band, corresponding to promotion of each of the three occupied valence p electrons of I^-, are computed.   Numerical convergence is achieved for all three components in a total of 380 snapshots. The energy gap with the ground anion state is histogramed; the band components are shown as black lines and the overall distribution of transition energies is shown in green. A Gaussian fit to the overall band shape (red) has FWHM = 0.49 eV.

References:

(1)   Blandamer, M.; Fox, M. *Chem. Rev.* **1970**, *70*, 59.

(2)   Jortner, J.; Treinin, A. *J. Chem. Soc. Farad. Trans.* **1962**, *58*, 1503.

(3)   Jortner, J.; Ottolenghi, M.; Stein, G. *J. Phys. Chem.* **1964**, *68*, 247.

(4)   Platzmann, R.; Franck, J. *Z. Physik.* **1954**, *138*, 411.

(5)   Jortner, J.; Levine, R.; Ottolenghi, M.; Stein, G. *J. Phys. Chem.* **1961**, *65*, 1232.

(6)   Franck, J.; Schiebe, G. *Z. Phys. Chem. A* **1928**, *139*, 22.

(7)   Hart, E. J.; Boag, J. W. *J. Am. Chem. Soc.* **1962**, *84*, 4090.

(8)   Kloepfer, J. A.; Vilchiz, V. H.; Lenchenkov, V. A.; Bradforth, S. E. *Chem. Phys. Lett.* **1998**, *298*, 120.

(9)   Kloepfer, J. A.; Vilchiz, V. H.; Lenchenkov, V. A.; Germaine, A. C.; Bradforth, S. E. *J. Chem. Phys* **2000**, *113*, 6288.

(10)   Vilchiz, V. H.; Kloepfer, J. A.; Germaine, A. C.; Lenchenkov, V. A.; Bradforth, S. E. *J. Phys. Chem. A* **2001**, *A 105*, 1711.

(11)   Kloepfer, J. A.; Vilchiz, V. H.; Lenchenkov, V. A.; Bradforth, S. E. Electron Photodetachment in Solution. In *Liquid Dynamics: Into the New Millennium*; Fourkas, J., Ed.; ACS Books: Washington, D.C., 2001.

(12)   Sheu, W.-S.; Rossky, P. J. *J. Phys. Chem.* **1996**, *100*, 1295.

(13)   Stein, G.; Treinin, A. *J. Chem. Soc. Farad. Trans.* **1959**, *55*, 1086.

(14)   Stein, G.; Treinin, A. *J. Chem. Soc. Farad. Trans.* **1959**, *55*, 1091.

(15)   Smith, M.; Symons, M. C. R. *Faraday Discuss. Chem. Soc.* **1957**, *24*, 206.

(16)   Smith, M.; Symons, M. C. R. *J. Chem. Soc. Farad. Trans.* **1958**, *54*, 346.

(17)   Rossky, P. J.; Schnitker, J. *J. Phys. Chem.* **1988**, *92*, 4277.

(18)   Horvath, O.; Stevenson, K. L. *Charge transfer photochemistry of coordination compounds*; VCH: New York City, NY, 1993.

(19)   Sheu, W.-S.; Rossky, P. J. *Chem. Phys. Lett.* **1993**, *213*, 233.

(20)   Sheu, W.-S.; Rossky, P. J. *Chem. Phys. Lett.* **1993**, *202*, 186.

(21)   Sheu, W.-S.; Rossky, P. J. *J. Am. Chem. Soc.* **1993**, *115*, 7729.

(22)   Borgis, D.; Staib, A. *Chem. Phys. Lett.* **1994**, *230*, 405.

(23)   Borgis, D.; Staib, A. *J. Chem. Phys.* **1996**, *104*, 4776.

(24)   Staib, A.; Borgis, D. *J. Chem. Phys.* **1996**, *104*, 9027.

(25)   Staib, A.; Borgis, D. *J. Chem. Phys.* **1995**, *103*, 2642.

(26)   Serxner, D.; Dessent, C. E. H.; Johnson, M. A. *J. Chem. Phys.* **1996**, *105*, 7231.

(27)   Lehr, L.; Zanni, M. T.; Frischkorn, C.; Weinkauf, R.; Neumark, D. M. *Science* **1999**, *284*, 635.

(28)   Kim, J.; Lee, H. M.; Suh, S. B.; Majumdar, D.; Kim, K. S. *J. Chem. Phys.* **2000**, *113*, 5259.

(29)   Majumdar, D.; Kim, J.; Kim, K. S. *J. Chem. Phys.* **2000**, *112*, 101.

(30)   Chen, H.-Y.; Sheu, W.-S. *J. Am. Chem. Soc.* **2000**, *122*, 7534.

(31)   Chen, H. Y.; Sheu, W. S. *Chem. Phys. Lett.* **2001**, *335*, 475.

(32)   Waterland, M.; Myers Kelley, A. *J. Phys. Chem. B* **2001**, *in press*.

(33)   Vila, F.; Jordan, K. D. *J. Phys. Chem. A* **2001**, *submitted*.

(34)   Dessent, C.; Kim, J.; Johnson, M. A. *Acc. Chem. Res.* **1998**, *31*, 527.

(35)   Chen, H.-Y.; Sheu, W.-S. *J. Chem. Phys.* **1999**, *110*, 9032.

(36)   Landman, U.; Barnett, R. N.; Cleveland, C. L.; Scharf, D.; Jortner, J. *J. Phys. Chem.* **1987**, *91*, 4890.

(37)   Gutowski, M.; Jordan, K. D.; Skurski, P. *J. Phys. Chem. A* **1998**, *102*, 2624.

(38)   Markovich, G.; Pollack, S.; Giniger, R.; Cheshnovsky, O. *Z. Phys. D* **1993**, *26*, 98.

(39)   Dang, L. X.; Garrett, B. C. *J. Chem. Phys.* **1993**, *99*, 2972.

(40)   Jungwirth, P.; Tobias, D. J. *J. Phys. Chem. B* **2001**, *submitted*.

(41)   Dang, L. X. *J. Phys. Chem. B* **2001**, *submitted*.

(42)   Coe, J. V.; Earhart, A. D.; Cohen, M. H.; Hoffman, G. J.; Sarkas, H. W.; Bowen, K. H. *J. Chem. Phys.* **1997**, *107*, 6023.

(43)   Combariza, J. E.; Kestner, N. R.; Jortner, J. *J. Chem. Phys.* **1994**, *100*, 2851.

(44)   LaJohn, L. A.; Christiansen, P. A.; Ross, R. B.; Atashroo, T.; Ermler, W. C. *J. Chem. Phys.* **1987**, *87*, 2812.

(45)   Hotop, H.; Lineberger, W. C. *J. Phys. Chem. Ref. Data* **1985**, *14*, 731.

(46)   Dang, L. X.; Rice, J. E.; Caldwell, J.; Kollman, P. A. *J. Am. Chem. Soc.* **1991**, *113*, 2481.

(47)   Pearlman, D. A.; Case, D. A.; Caldwell, J. W.; Ross, W. S.; Cheatham, T. E.; DeBolt, S. E.; Ferguson, D. M.; Siebel, G. L.; Kollman, P. A. *Comput. Phys. Commun.* **1995**, *91*, 1.

(48)   Dang, L. X. *J. Chem. Phys.* **1999**, *110*, 1526.

(49)   Markovich, G.; Perera, L.; Berkowitz, M. L.; Cheshnovsky, O. *J. Chem. Phys.* **1996**, *105*, 2675.

(50)   Essmann, U.; Perera, L.; Berkowitz, M. L.; Darden, T.; Pedersen, L. G. *J. Chem. Phys.* **1995**, *103*, 8577.

(51)   Warshel, A. *J. Phys. Chem.* **1979**, *83*, 1640.

(52)   Berendsen, H. J. C.; Grigera, J. R.; Straatsma, T. P. *J. Phys. Chem.* **1987**, *91*, 6269.

(53)   Frisch, M. J.; Trucks, G. W.; Schlegel, H. B.; Scuseria, G. E.; Robb, M. A.; Cheeseman, J. R.; V. G. Zakrzewski; Montgomery, J. A.; Stratmann, R. E.; Burant, J. C.; Dapprich, S.; Millam, J. M.; Daniels, A. D.; Kudin, K. N.; Strain, M. C.; O. Farkas; Tomasi, J.; Barone, V.; Cossi, M.; Cammi, R.; Mennucci, B.; C. Pomelli; Adamo, C.; Clifford, S.; Ochterski, J.; Petersson, G. A.; Ayala, P. Y.; Cui, Q.; Morokuma, K.; Malick, D. K.; Rabuck, A. D.; Raghavachari, K.; Foresman, J. B.; Cioslowski, J.; Ortiz, J. V.; Stefanov, B. B.; Liu, G.; Liashenko, A.; Piskorz, P.; Komaromi, I.; Gomperts, R.; Martin, R. L.; Fox, D. J.; Keith, T.; Al-Laham, M. A.; Peng, C. Y.; Nanayakkara, A.; Gonzales, C.; Challacombe, M.; Gill, P. M. W.; Johnson, B. G.; Chen, W.; Wong, M. W.; Andres, J. L.; Head-Gordon, M.; Replogle, E. S.; Pople, J. A. Gaussian98; Gaussian Inc.: Pittsburgh, PA, 1998.

(54)   Case, D. A.; Pearlman, D. A.; Caldwell, J. W.; III, T. E. C.; Ross, W. S.; Simmerling, C. L.; Darden, T. A.; Mertz, K. M.; Stanton, R. V.; Cheng, A. L.; Vincent, J. J.; Crowley, M.; Tsui, V.; Radmer, R. J.; Duan, Y.; Pitera, J.; Massova, I.; Seibel, G. L.; Singh, U. C.; Weiner, P.; Kollman, P. A. Amber6; University of California, San Francisco: San Francisco, CA, 1999.

(55)   Takahashi, N.; Sakai, K.; Tanida, H.; Watanabe, I. *Chem. Phys. Lett.* **1995**, *246*, 183.

(56)   Watanabe, I.; Takahashi, N.; Tanida, H. *Chem. Phys. Lett.* **1998**, *287*, 714.

(57)   Miertus, S.; Tomasi, J. *Chem. Phys.* **1982**, *65*, 239.

(58)   Christiansen, O.; Nymand, T. M.; Mikkelsen, K. V. *J. Chem. Phys.* **2000**, *113*, 8101.

(59)   Luzhkov, V.; Warshel, A. *J. Am. Chem. Soc.* **1991**, *113*, 4491.

(60)   Liu, Y. P.; Newton, M. D. *J. Phys. Chem.* **1995**, *99*, 12382.

(61)   Christiansen, O.; Mikkelsen, K. V. *J. Chem. Phys.* **1999**, *110*, 8348.

(62)   Ohtaki, H.; Radnai, T. *Chem. Rev.* **1993**, *93*, 1157.

(63)   Griffiths, T. R.; Symons, M. C. R. *J. Chem. Soc. Farad. Trans.* **1960**, *56*, 1125.

(64)   Kohno, J.; Mafune, F.; Kondow, T. *J. Phys. Chem. A* **2001**, *105*, 5990.

(65)   Jungwirth, P.; Tobias, D. J. *J. Phys. Chem. A* **2001**, *submitted*.

(66)   Ellison, F. O. *J. Am. Chem. Soc.* **1963**, *85*, 3540.

(67)   Krylov, A. I.; Gerber, R. B. *J. Chem. Phys.* **1997**, *106*, 6574.

(68)   Tran, V.; Schwartz, B. *J. Phys. Chem. B* **1999**, *103*, 5570.

(69)   Figures refer to model 1 favored by of Ref. [21].

(70)   Jou, F.-Y.; Freeman, G. R. *J. Phys. Chem.* **1979**, *83*, 2383.

(71)   Yokoyama, K.; Silva, C.; Son, D. H.; Walhout, P. K.; Barbara, P. F. *J. Phys. Chem. A* **1998**, *102*, 6957.

(72)   Schwartz, B. J.; Rossky, P. J. *J. Chem. Phys.* **1994**, *101*, 6917.

(73)   Baltuska, A.; Emde, M. F.; Pshenichnikov, M. S.; Wiersma, D. A. *J. Phys. Chem. A* **1999**, *103*, 10065.

(74)   Wang, Z.; Shoshana, O.; Ruhman, S. Probing CTTS dynamics of Na^- in THF - novel relaxation and polarization effects. In *Ultrafast Phenomena XII*; Elsaesser, T., Mukamel, S., Murnane, M. M., Scherer, N. F., Eds.; Springer Verlag: Berlin, 2000.

(75)   Crowell, R. A.; Bartels, D. M. *J. Phys. Chem.* **1996**, *100*, 17940.

(76)   Kee, T. W.; Son, D. H.; Kambhampati, P.; Barbara, P. F. *J. Phys. Chem. A* **2001**, *in press*.

(77)   Kloepfer, J. A.; Vilchiz, V. H.; Chen, X.; Bradforth, S. E. *J. Chem. Phys.* **2001**, *submitted*.
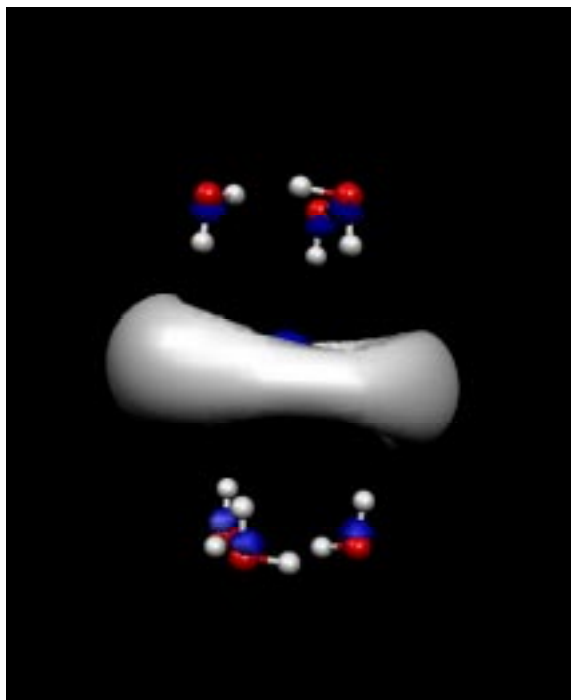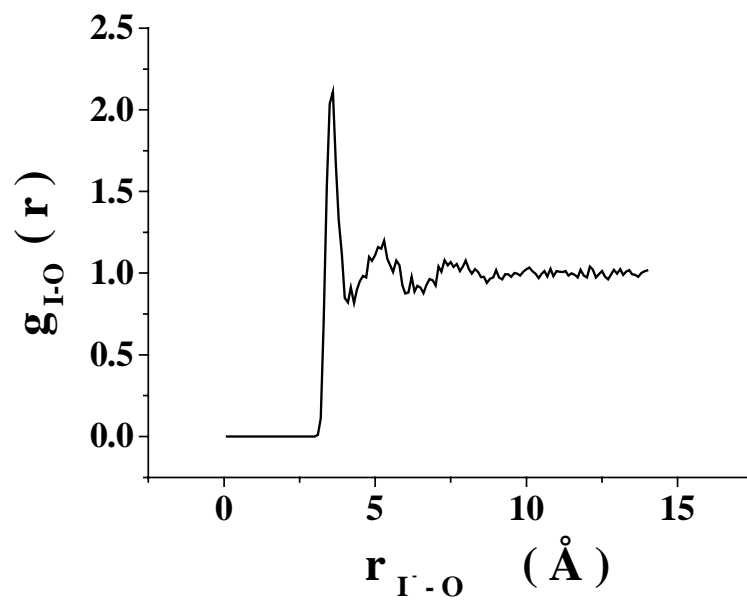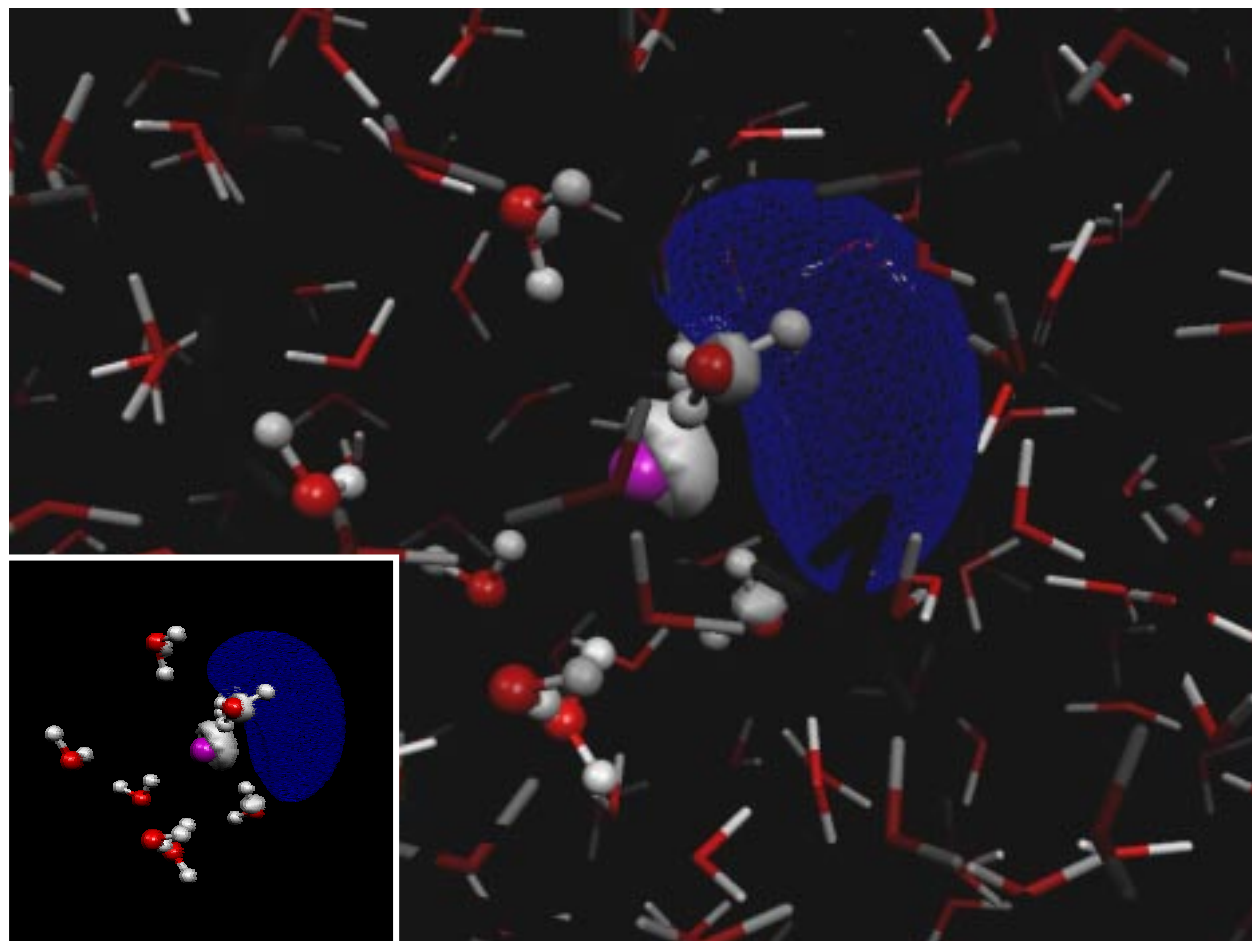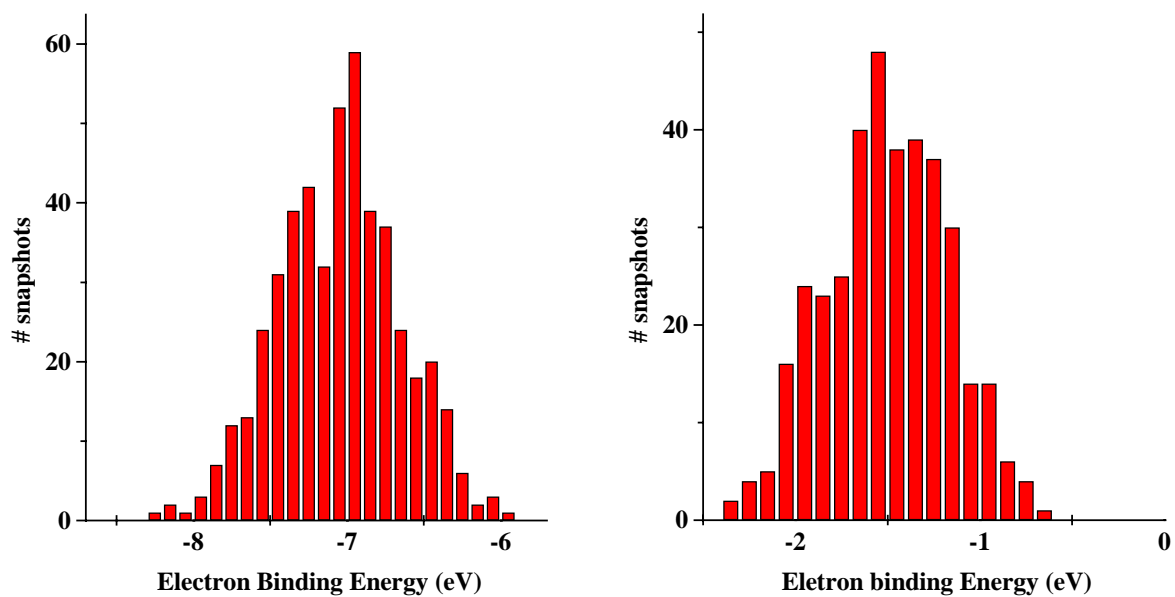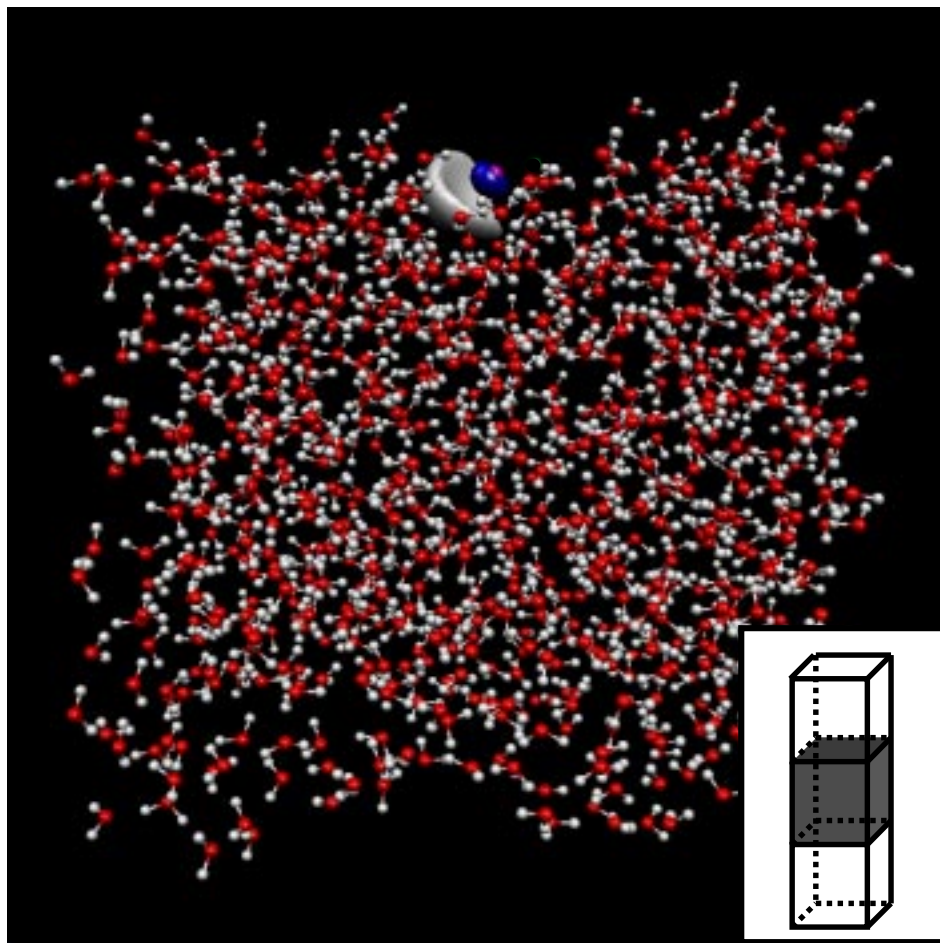
Figure 1

Figure 2

Bradforth and Jungwirth
The excited states of iodide anions in water…

Figure 3

Bradforth and Jungwirth
The excited states of iodide anions in water…

Figure 4

Figure 5

Figure 6

Bradforth and Jungwirth
The excited states of iodide anions in water…